Electronic Supplementary Material (ESI) for Physical Chemistry Chemical Physics.

Supporting Information

Kinetics of DNA duplex formation: A-tracts *versus* AT-tracts

Jean Ann Wyer, Mads Bejder Kristensen, Nykola C. Jones, Søren Vrønning Hoffmann and Steen Brøndsted Nielsen

---

Absorption spectra of single strands and duplexes

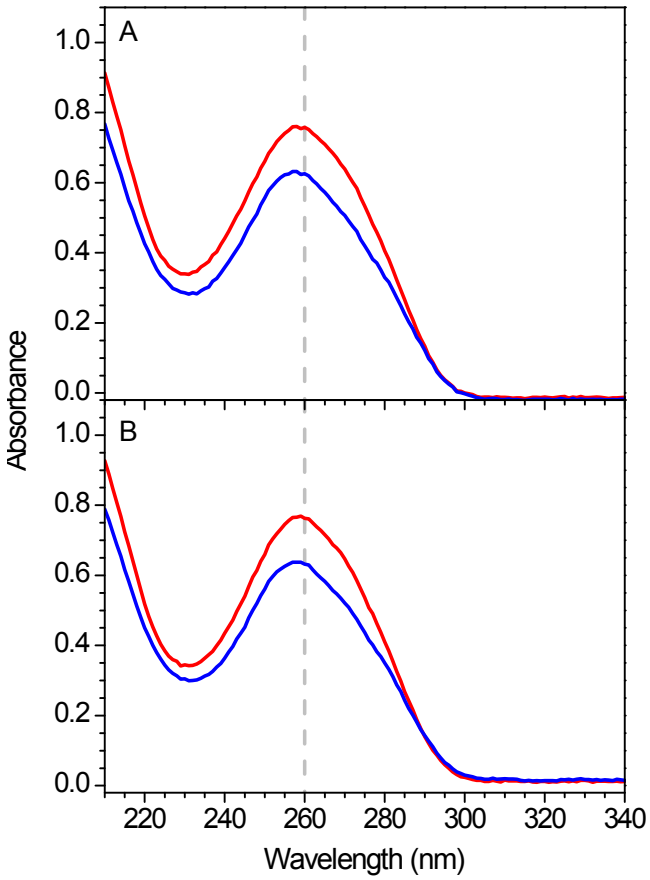

Fig S1: (A) The sum of the absorbances of the single strands $\mathbf{A_S}$**-a** (2.5 μM) and $\mathbf{A_S}$**-b** (2.5 μM) in a 10 mM phosphate buffer (pH 7.0), 100 mM NaCl solution (red line) and the absorbance of the duplex formed between them (blue line). (B) The sum of the absorbances of the single strands $\mathbf{A_L}$**-a** (2.0 μM) and $\mathbf{A_L}$**-b** (2.0 μM) in a 10 mM phosphate buffer (pH 7.0), 100 mM NaCl solution (red line) and the absorbance of the duplex formed between them (blue line).

Kinetics data for pairs I and II and results from modelling calculations (structures)

The absorbances at 260 nm over time associated with the formation of pair **I** and pair **II** at 30°C are shown as examples in Fig. S2. The hybridisation times are clearly different with pair **II** being faster than pair **I** in agreement with the previous work.

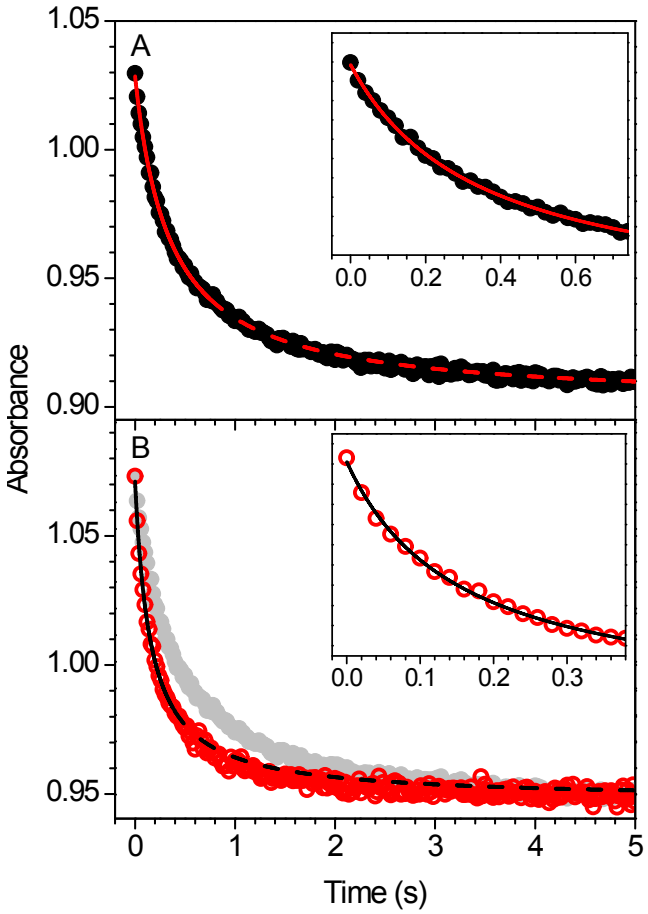

Fig S2: Time course of the absorbance at 260 nm associated with duplex formation between (A) 4.3 μM of strands **Ia** and **Ib** and (B) 4.4 μM of strands **IIa** and **IIb** at 30ºC. A second-order equation was fit to the same absorbance change (70% of the total change) in each, namely the first 0.74 s and 0.38 s, respectively. Dotted lines show the fits extended over the full timescale and expanded views of the fitted data points are shown as insets. The data points from A scaled relative to the data in B are shown in B for comparison purposes as grey solid circles.

Rate constants at each temperature were determined using two different methods, 1: fitting the data with a second-order equation and 2: fitting the initial data with a linear function (see main text for further details on the fitting processes). Arrhenius plots of the resulting data are shown in Fig. S3. It is seen that for both methods our results for pair **I** agree quantitatively with those from the previous work, while for pair **II** the agreement is good except at 35°C. However, as the melting temperature of the duplex is 38.6°C (calculated using the method described in Ref. 53 and references therein) not all of the strands at 35°C form duplexes, which implies that the models do not describe the data well at this temperature (melting is not accounted for). The activation energies for the formation

of pair **I** are found to be 44.5 ± 7.2 kJ mol^{-1} and 36.2 ± 8.9 kJ mol^{-1} for methods 1 and 2, respectively, while that reported previously was 42.3 ± 4.8 kJ mol^{-1}, which is in between our two values.[4] For pair **II** our value for the activation energy deviates from that measured previously due to the discrepancy at 35°C; values of 7.5 ± 6.4 kJ mol^{-1} and 4.3 ± 4.9 kJ mol^{-1} were found using methods 1 and 2, respectively while that reported previously was 20.5 ± 1.5 kJ mol^{-1}.[4] However, activation energies of 17.6 ± 5.5 kJ mol^{-1} and 15.7 ± 3.7 kJ mol^{-1} are obtained for methods 1 and 2, respectively, if the point at 35°C is excluded.

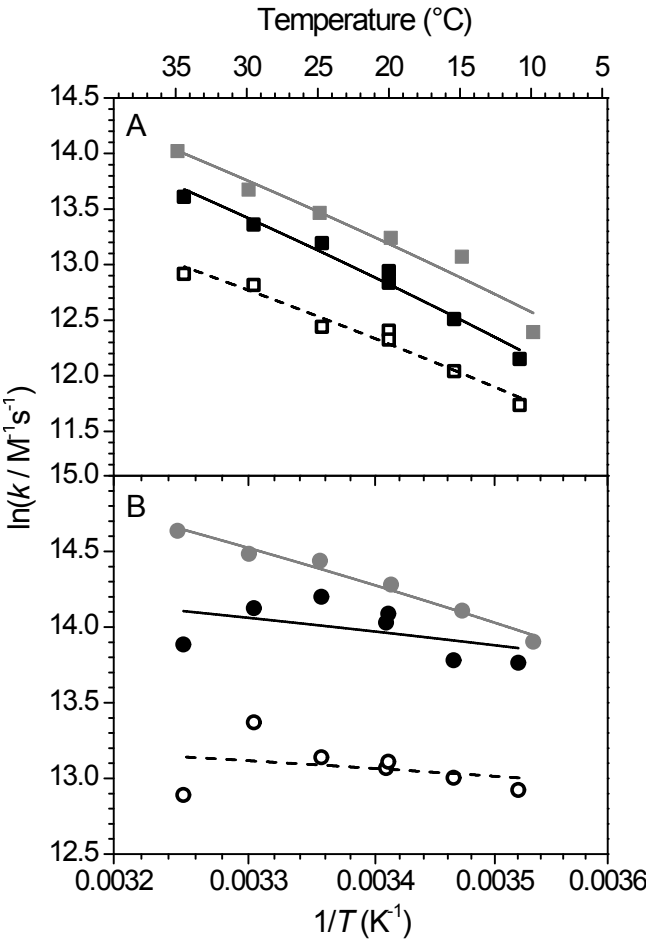

Fig S3: Arrhenius plots for the complexation of 4 μM of strands (A) **Ia** and **Ib** and (B) **IIa** and **IIb**. Solid black symbols: values for *k* found from second-order fits to a 70% drop in absorbance (method 1). Open black symbols: values for *k* found from linear fits to the initial data (method 2). Grey symbols: ref. [4]. The activation energies for the complexation of **Ia** and **Ib**, and **IIa** and **IIb** were found to be 44.5 ± 7.2 kJ mol^{-1} and 7.5 ± 6.4 kJ mol^{-1} for method 1 and 36.2 ± 8.9 kJ mol^{-1} and 4.3 ± 4.9 kJ mol^{-1} for method 2, respectively, while those reported previously were 42.3 ± 4.8 kJ mol^{-1} and 20.5 ± 1.5 kJ mol^{-1}.[4]

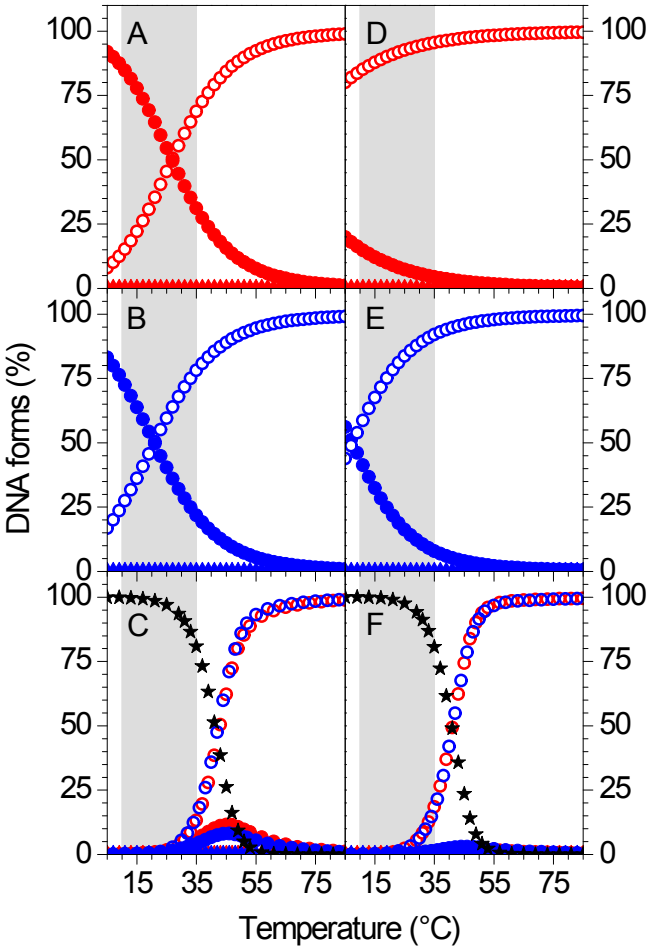

Fig S4: Simulated percentages of DNA in the different forms for strands **Ia**, **Ib**, **IIa** and **IIb** in 0.1 M Na^+ solutions as a function of temperature obtained using the UNAFold software package. Concentrations were (A) 8.0 μM of **Ia**, (B) 8.0 μM of **Ib**, (C) 4.0 μM of **Ia** with 4.0 μM of **Ib**, (D) 8.0 μM of **IIa**, (E) 8.0 μM of **IIb**, and (F) 4.0 μM of **IIa** with 4.0 μM of **IIb**. Data for the unfolded single strands (●), folded single strands (hairpins) (ᔓ), homo-duplexes (□) and hetero-duplexes (★) are plotted for **Ia** (red symbols) and **Ib** (blue symbols) in the left column and **IIa** (red symbols) and **IIb** (blue symbols) in the right. The experimental range is highlighted in grey.

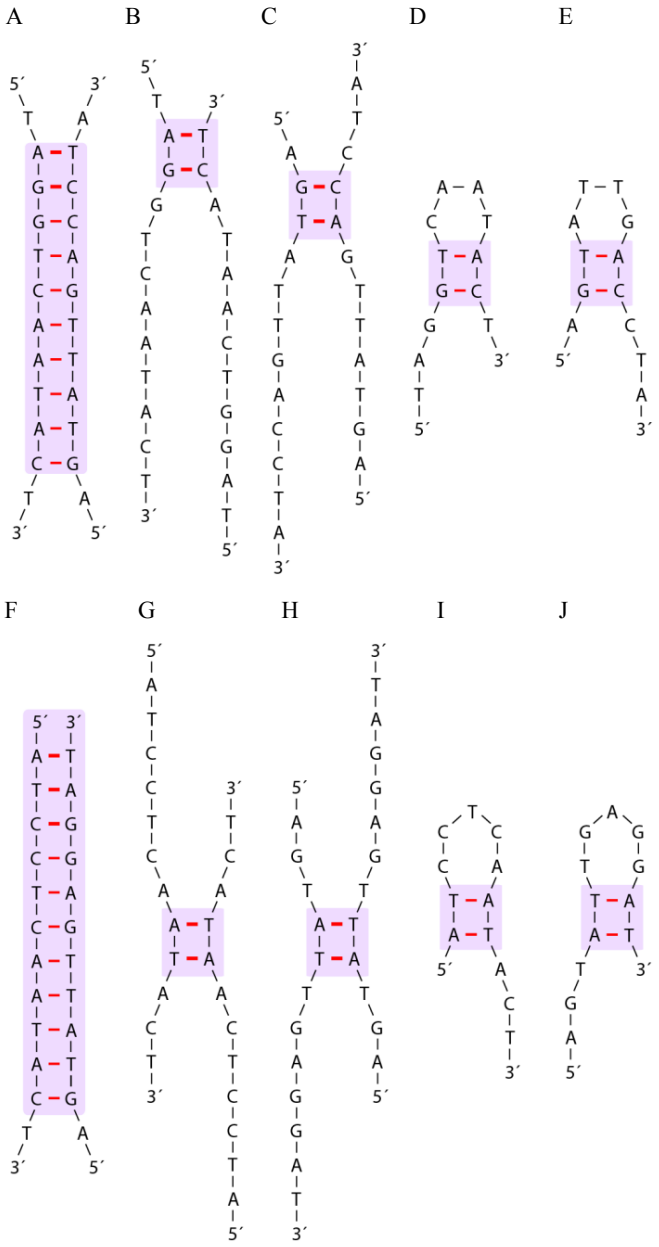

Fig S5: Calculated minimum energy structures at room temperature (25°C) for (A) the hetero-duplex between **Ia** and **Ib**; (B) the homo-duplex for **Ia**; (C) the homo-duplex for **Ib**; (D) the hairpin of **Ia**; (E) the hairpin of **Ib**; (F) the hetero-duplex between **IIa** and **IIb**; (G) the homo-duplex for **IIa**; (H) the homo-duplex for **IIb**; (I) the hairpin of **IIa**; (J) the hairpin of **IIb**. Note: Regions of complexation are highlighted.

Absorbance and CD data at different temperatures for separate solutions of AT_s-a and AT_s-b

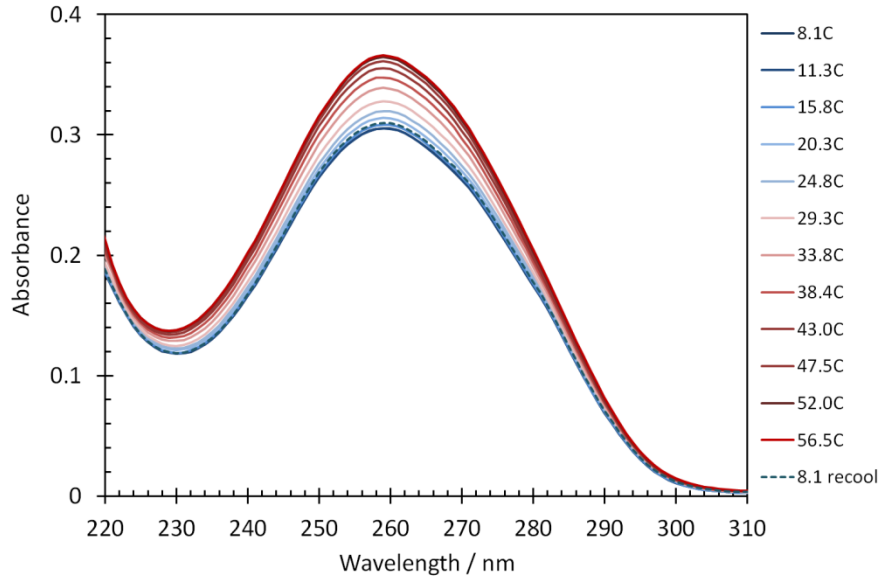

Fig S6: Absorption spectra of **AT_s-a** recorded at the AU synchrotron radiation facility at various temperatures.

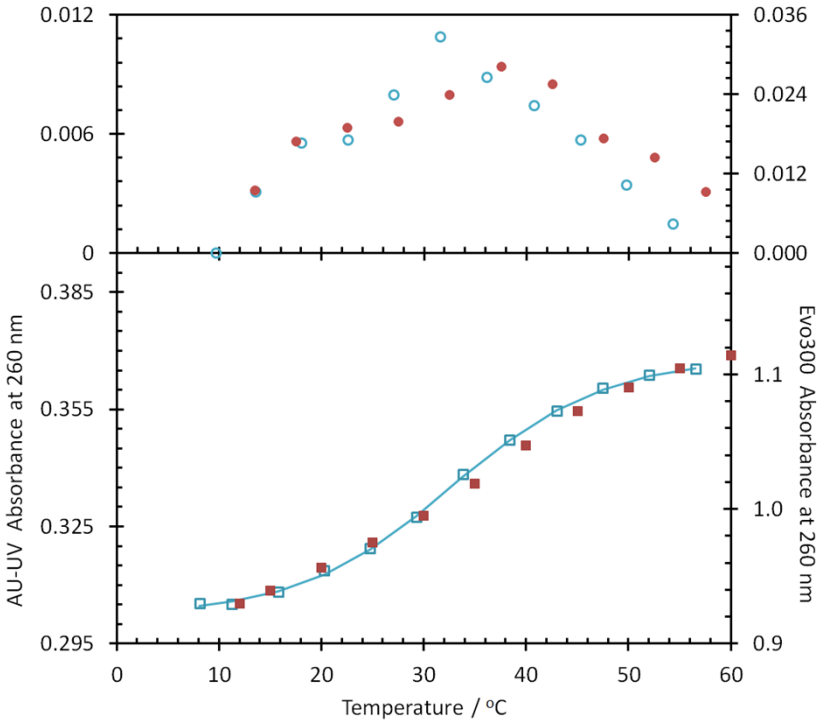

Fig S7: Bottom: Absorption at 260 nm by **AT_s-a** *versus* temperature recorded with a commercial EVO300 spectrophotometer (right axis) and at the AU synchrotron radiation facility (left axis). The concentration of DNA strands is a factor of three lower in the latter case. Top: The change in absorbance per °C.

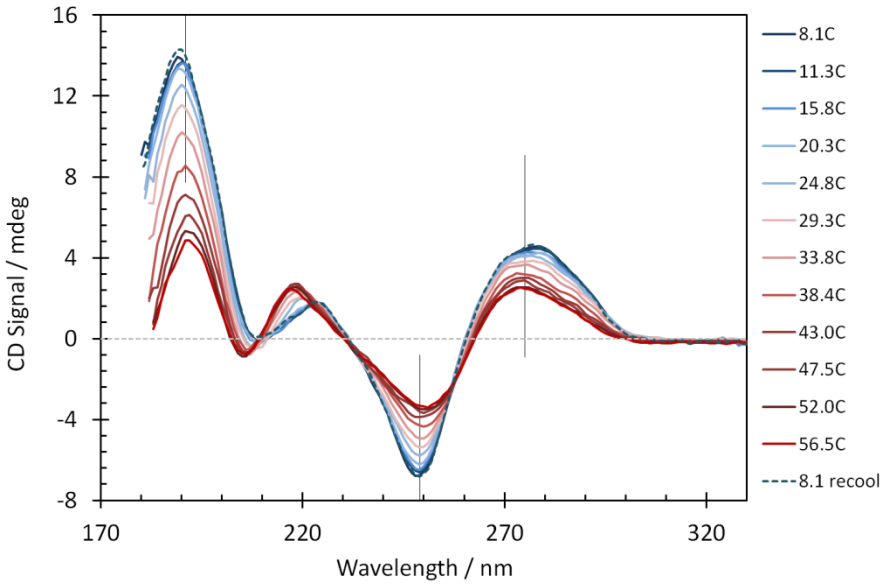

Fig S8: CD spectra of **AT$_s$-a** recorded at the AU synchrotron radiation facility at various temperatures.

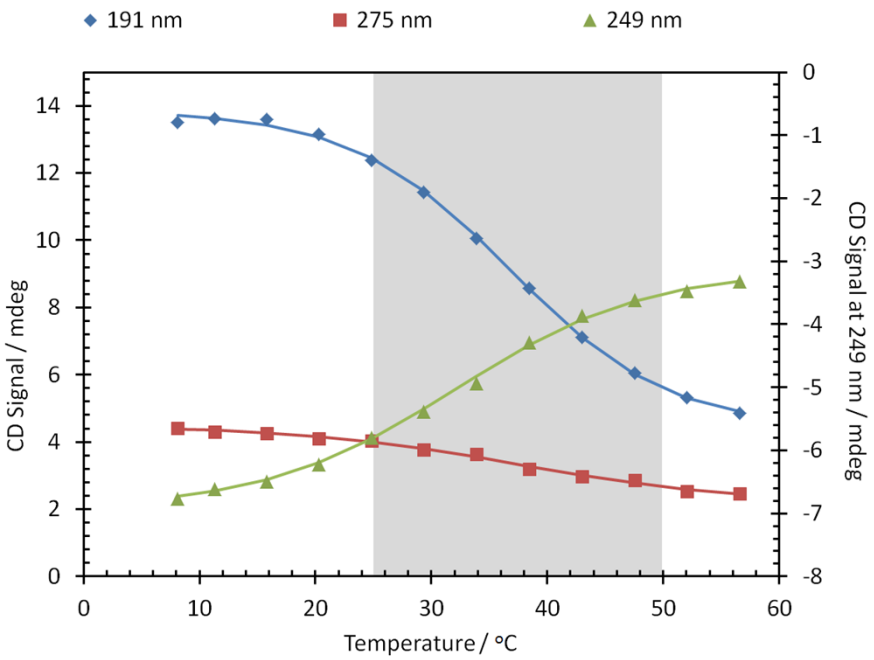

Fig S9: CD signals of **AT$_s$-a** at 191 nm, 249 nm, and 275 nm *versus* temperature. The grey area is where the largest changes occur.

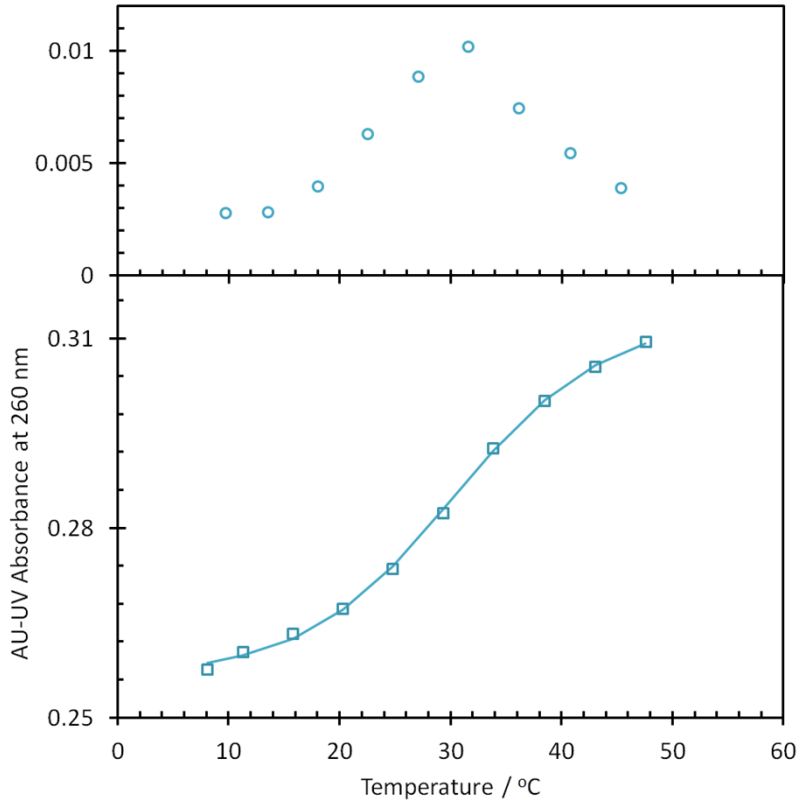

Fig S10: Bottom: Absorption at 260 nm by **AT$_s$-b** *versus* temperature recorded at the AU synchrotron radiation facility. The change in absorbance per °C.

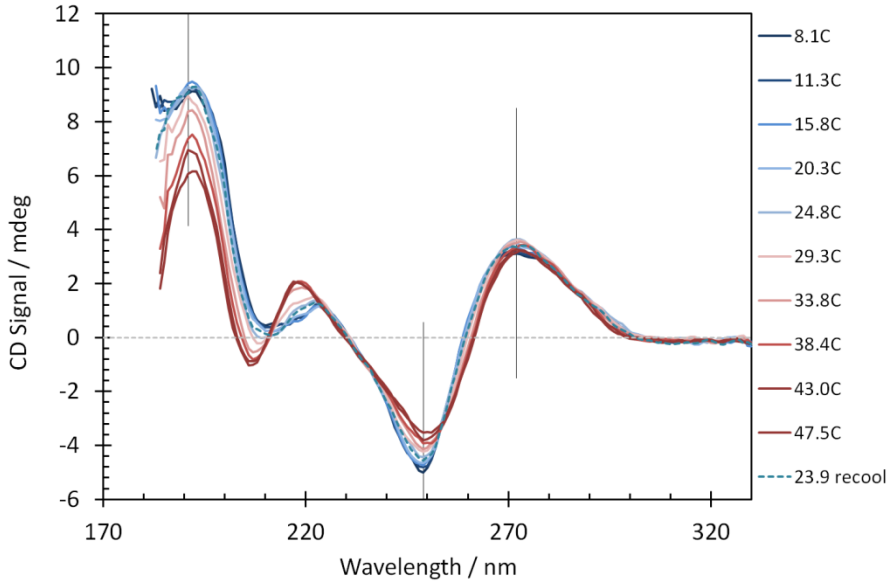

Fig S11: CD spectra of **AT$_s$-a** recorded at the AU synchrotron radiation facility at various temperatures.

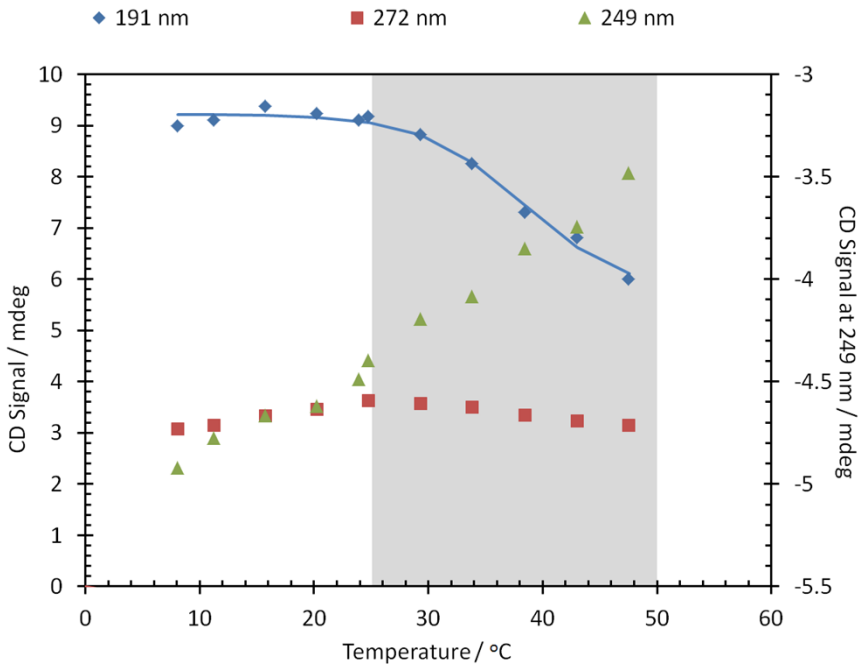

Fig S12: CD signals of **AT$_s$-b** at 191 nm, 249 nm, and 272 nm *versus* temperature. The grey area is where the largest changes occur.